

The submitted manuscript has been authored by a contractor of the U. S. Government under contract No. W-31-109-ENG-38. Accordingly, the U. S. Government retains a nonexclusive, royalty-free license to publish or reproduce the published form of this contribution, or allow others to do so, for U. S. Government purposes.

ANL/TD/CP--83462
Conf-941129--9

EVALUATION OF NEUTRON TECHNIQUES FOR ILLICIT SUBSTANCE DETECTION

C. L. FINK, B. J. MICKLICH, T. J. YULE, P. HUMM, L. SAGALOVSKY and M. M. MARTIN
Technology Development Division, Argonne National Laboratory, Argonne, Illinois 60439 USA

We are studying inspection systems based on the use of fast neutrons for detecting illicit substances such as explosives and drugs in luggage and cargo containers. Fast neutron techniques can determine the quantities of light elements such as carbon, nitrogen, and oxygen in a volume element. Illicit substances containing these elements are characterized by distinctive elemental densities or density ratios. We discuss modeling and tomographic reconstruction studies for fast-neutron transmission spectroscopy.

1. Introduction

Nuclear techniques using fast neutrons are being examined for detection of illicit substances, such as explosives and drugs, in luggage and cargo containers. Fast neutron techniques are attractive because they can determine the quantities of many of the light elements of interest, such as carbon, nitrogen, and oxygen. We are currently analyzing two system concepts: fast-neutron transmission spectroscopy FNTS and pulsed fast-neutron analysis PFNA [1]. In this paper we discuss only FNTS as applied to the detection of explosives in luggage.

FNTS is based on the fact that many of the light elements of interest have significant features in their cross sections that allow identification of the elemental constituents from the measured transmission ratio. The technique was first examined by Overlay [2] to determine compositions of bulk organic materials. In this technique an accelerator is used to produce nanosecond pulsed beams of protons or deuterons that strike a target and produce a pulsed beam of neutrons with a continuum of energies. The material to be interrogated is placed in the flight path between the target and detector and time-of-flight techniques are used to measure a transmission ratio as a function of neutron energy. This ratio is unfolded to yield the projected areal densities of the various elements. In this paper we investigate the use of FNTS in detecting a block of RDX explosive with relatively poor pixel resolution, 3 to 5 projections, and realistic errors in the unfolded projection data.

2. Monte Carlo Modeling

The phantom used in this study is shown in Fig. 1. It consists of an 8-cm square of RDX explosive

($C_3H_6N_6O_6$, $\rho = 1.83 \text{ g/cm}^3$), an 8-cm square of nylon ($C_6H_{11}NO$, $\rho = 1.1 \text{ g/cm}^3$), an 8-cm diameter circle of ethanol (C_2H_5OH , $\rho = 0.789 \text{ g/cm}^3$), and a uniform background of silk ($C_3H_{11}N_3O_6$, $\rho = 0.3 \text{ g/cm}^3$) placed inside a 40-cm square. An 8-cm cube of RDX corresponds to approximately 1 kg of explosive. If the slice used in this reconstruction is assumed to be 2 cm thick, then the RDX object has a mass of 230 g. If the elements from the other objects were converted into RDX explosive, approximately 900 g of explosive could be formed.

The Monte Carlo transport code MCNP [3] was used to simulate neutron transmission through the phantom. The calculational model assumes a white neutron source (the zero-degree neutron energy spectrum from the $^9\text{Be}(d,n)$ reaction at $E_d = 5 \text{ MeV}$) illuminating the object being interrogated with a collimated, parallel neutron beam which is 2 cm by 2 cm in cross section. This source has a high neutron yield in the range 1-4 MeV, which contains many resolved resonances for the light elements. The source-detector distance was 5 m, with source and detector timing widths of 2 ns. Analog particle transport was used (i.e., no variance reduction) so that each neutron from the source represents one neutron from a real source. This results in counting statistics that have the same magnitude and variation across energy phase space as would be seen in an actual experimental or test geometry. Use of the appropriate errors is important in evaluating analysis and decision-making algorithms that use the unfolded projection data.

The transmission data are analyzed in the time domain using standard nuclear techniques [4] adapted to the method of effective variance [5]. The details of the algorithm are contained in References [6] and [7]. A sample transmission spectrum for bin 9 at 0° (which passes through the RDX and nylon

MASTER

DISTRIBUTION OF THIS DOCUMENT IS UNLIMITED

875

✓

squares from left to right) is shown in Fig. 2. The results of unfolding this spectrum are shown in Table 1.

Table 1. Exact and unfolded results for bin 9, 0° projection through the 3-body phantom of Figure 1.

element	exact #/cm ² (10 ²⁴)	unfolded #/cm ² (10 ²⁴)
H	1.707	1.034 ± 0.111
C	0.470	0.507 ± 0.055
N	0.355	0.339 ± 0.102
O	0.425	0.440 ± 0.035
F	0	-0.0365 ± 0.0863
Al	0	0.0025 ± 0.0818
Si	0	0.0203 ± 0.0447
Cl	0	-0.0311 ± 0.1206
Fe	0	-0.0165 ± 0.0969
Cu	0	0.0249 ± 0.0858

3. Tomography and Explosive Detection

The experimental data measured by FNTS will consist of one-dimensional projection profiles of the areal density of the elements H, C, N, and O at one or more projection angles. The data from these projection profiles may be used directly or may undergo additional processing (e.g. tomographic reconstruction) before being input to an explosive detection algorithm.

The problem with the use of a single projection in explosive detection occurs because the projection data consists of an integral along the line-of-sight of the projection. Thus elements at different positions along this line-of-sight can overlap with the explosive and obscure the explosive signature when present, or combine with other elements to indicate the presence of explosives when no explosive is present. A single projection may be used as an initial screening to eliminate some luggage, however. For example, if insufficient nitrogen is detected in the projection data, then the presence of nitrogen based explosives can be excluded. Most suitcases will contain too much nitrogen in nonexplosive components to allow this simple algorithm to be used for more than an initial screening.

Thus we assume that any practical explosive detection technique will have to provide some spatial separation between suitcase objects. In this paper we investigate the use of tomographic techniques to provide this separation. Since the time for explosive

interrogation is limited, we will look at tomographic techniques that can provide reasonable results with a small number of projections. Reasonable in this case is not necessary a high-fidelity reconstruction but rather a reconstruction that provides enough separation between objects to maximize the success rate of an explosive detection algorithm.

Some parameters that impact on explosive detection are (1) the number of projection angles, (2) the pixel resolution, (3) the shape and size of the explosive, (4) the position, shape, and type of obscuring material, (5) the reconstruction algorithm, (6) the accuracy with which the elemental projection densities can be obtained, and (7) the qualifier used to detect explosive. The emphasis in this paper is on the number of projections required to detect a relatively large block of RDX sampled with relatively poor pixel resolution using realistic uncertainties in the elemental areal densities.

4. Few-View Reconstruction

We have used the tomographic reconstruction techniques contained in the Donner library [8] to study the phantom of Fig. 1. For reconstructions using a small number of projections, the algebraic reconstruction technique provided the best reconstruction. In particular, we have looked at conjugate gradient, maximum likelihood [9], and maximum entropy techniques. In general all three techniques produced a reasonable reconstruction of the phantom. For simplicity, we choose to use the maximum likelihood method with 25 iterations.

Fig. 3 shows a reconstruction of the nitrogen density distribution for 3 and 5 projection angles starting at 0 degrees (horizontal projection) and uniformly distributed between 0 and 180 degrees. The results show that the 5-angle reconstruction provides a better image of the square and of the actual nitrogen density. The 3-angle reconstruction is not that inferior, however, and could provide a sufficiently accurate reconstruction of the nitrogen density distribution to be used successfully by various explosive qualifiers.

5. Reconstruction with MCNP Data

The results shown in Fig. 3 use projection data calculated directly from the phantom density distribution. In practice, the projection data will have uncertainties from the statistics of the projection process and from the unfolding of the density distributions from the measured neutron spectra.

DISCLAIMER

Portions of this document may be illegible in electronic image products. Images are produced from the best available original document.

We have used MCNP and the unfolding process described in Section 2 to calculate the projections for the case of 3 and 5 angles. The results are shown in Fig. 4 for the nitrogen density distribution. A side-by-side comparison shows that reconstructed results from the MCNP study compare favorably to those using the exact projections with no errors. Both the general shape and densities are reasonably reproduced.

6. An Explosive Detection Algorithm

The purpose of the tomographic reconstruction is to spatially separate objects within the phantom to avoid confusing the explosive qualifier when it is applied to each pixel in testing for the presence or absence of explosives. The best explosive qualifier is one that is sensitive to explosives and relatively insensitive to other materials and combination of materials that might occur because of pixel resolution, reconstruction error, or statistical uncertainty.

In this paper we use an explosive qualifier that converts the H, C, O, and N elemental densities at each pixel into an equivalent explosive density. Thus the higher the density the more likely that the pixel contains an explosive.

The top half of Fig. 4 shows the result of applying this qualifier to the MCNP data for the case of 3 projection angles. Even for this small number of projections, and even though the exact shape is not very well resolved, the explosive is clearly visible. The bottom half of Fig. 4 shows the results if only pixels with explosive densities greater than 0.5, 1.0 and 1.5 are displayed. The 0.5 threshold overestimates the explosive area, while the 1.5 threshold underestimates it. For this case a density of 1.0 provides a good compromise between detection and false alarms.

7. Summary

The results of this work show that for the phantom used in these calculations, it is relatively easy to identify the square block of nitrogen-based explosive using three projection angles, 2-cm resolution, and reasonable uncertainty in the unfolded projection densities. Thus the FNTS appears to be a very promising method for explosive detection.

The next steps in this study involve looking at phantoms consisting of rectangular blocks of explosives in configuration with other types of

objects, and phantoms containing thin slabs of explosive. It is expected that the thin slab cases will impose more stringent requirements on the number of projections and on the pixel resolution. We also intend to explore other explosive qualifiers.

Acknowledgments

This work was supported by the Federal Aviation Administration Technical Center under contract DTFA03-03-X-00021. We would like to thank Dr. Curtis Bell of the FAA for support and advice on this project. P. Humm and M. Martin were supported by the Student Research Participation Program of Argonne's Division of Educational Programs

References

- [1] T. J. Yule, B. J. Micklich, C. L. Fink, and D. L. Smith, Proc. 4th Int'l Conf. on Applications of Nuclear Techniques, Crete, Greece (June 1994).
- [2] J. C. Overley, Int. J. Appl. Radiat. Isot. 36 (1985); J. C. Overley, *Nucl. Instr. Meth. B24/25*, (1987) pp. 1058-1062.
- [3] J. Breisemeister, ed., "MCNP - A Generalized Monte Carlo Code for Neutron and Photon Transport, Version 3A," LA-7396-M, Rev. 2, Los Alamos National Laboratory (Sept. 1986).
- [4] D. L. Smith, ANL/NDM-62 (Nov. 1982).
- [5] J. Orear, *Amer. J. Phys.* 50, (1982) pp. 912-916.
- [6] B. J. Micklich, M. K. Harper, L. Sagalovsky, and D. L. Smith, Int'l Conf. on Nuclear Data for Science and Technology, Gatlinburg, TN (May 1994).
- [7] D. L. Smith, L. Sagalovsky, B. J. Micklich, M. K. Harper, and A. H. Novick, Proc. 4th Int'l Conf. on Applications of Nuclear Techniques, Crete, Greece (June 1994).
- [8] R. H. Huesman, G. T. Gullberg, W. L. Greenberg, T. F. Budinger, "RECLBL Library Users Manual : Donner Algorithms for Reconstruction Tomography," Lawrence Berkeley Laboratory Pub. 214, October 1977.
- [9] L. Zeng, Private Communication, University of Utah.

Figures

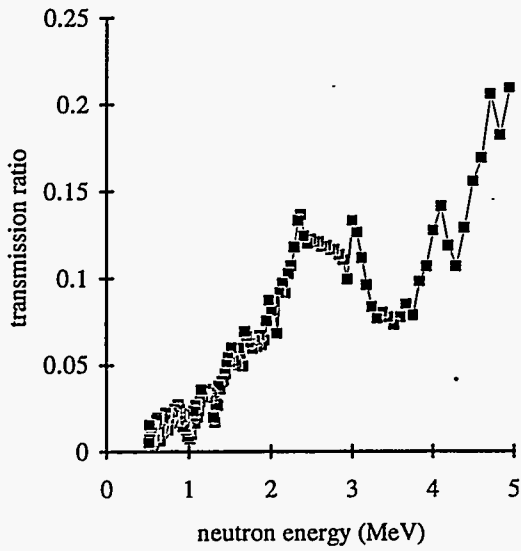


Fig. 2. Neutron transmission ratio as a function of energy for bin 9 of the 0° projection through the phantom of Fig. 1.

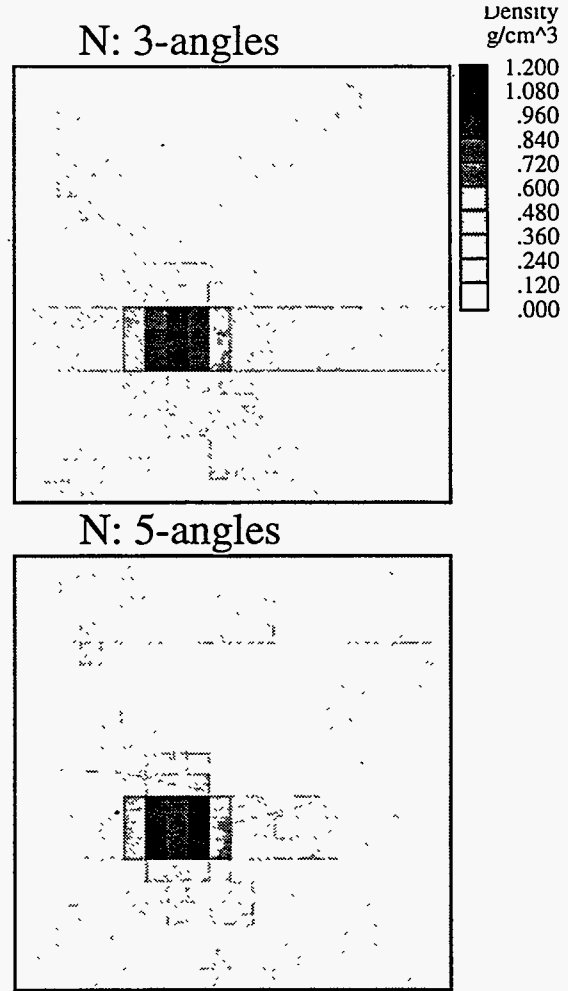


Fig. 3. Reconstruction of the nitrogen density distribution from 3 and 5 projections

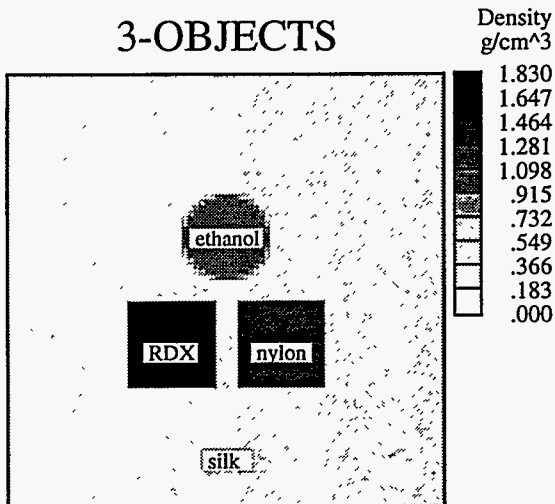
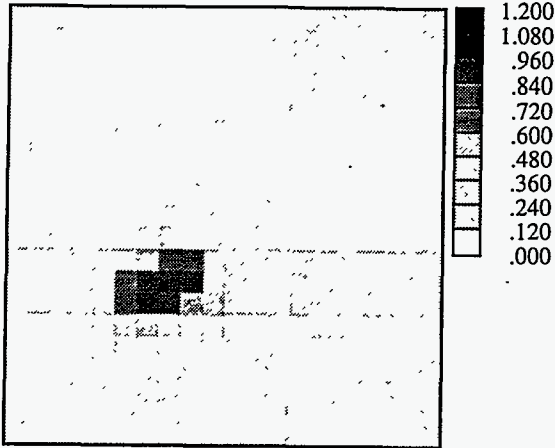
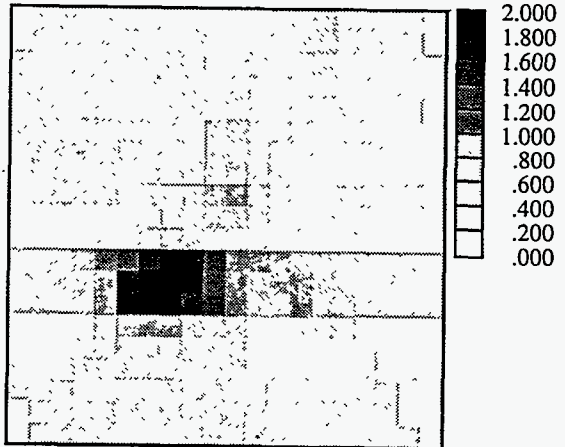


Fig. 1. Phantom used in these calculations. The pixel resolution in this picture is 0.5 cm. The resolution used in the reconstruction and MCNP calculations was 2.0 cm.

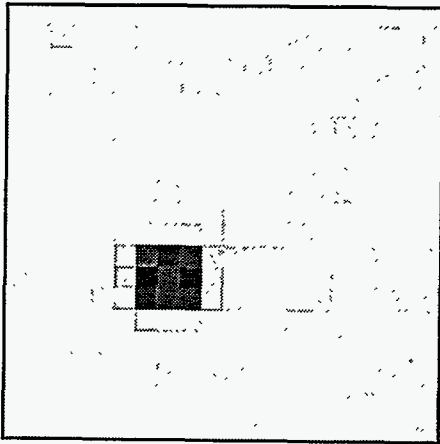
N: 3-angles - MCNP



EX: 3-angles - MCNP



N: 5-angles - MCNP



EB: 3-angles - MCNP

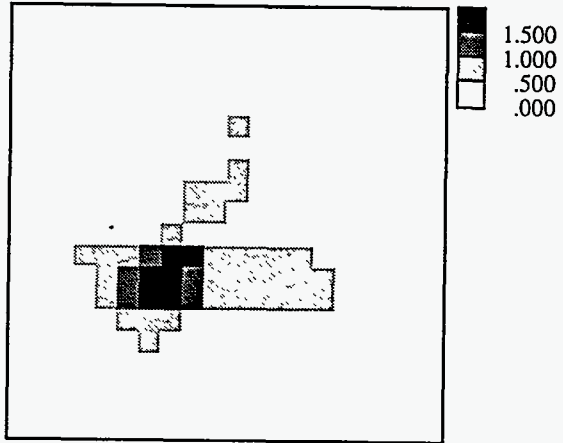


Fig. 4. Reconstruction of the nitrogen density distribution using the MCNP calculated projection data.

Fig. 5. The top half shows the 2-D density distribution of the explosive qualifier described in Section 6. The bottom half shows those pixels that have a qualifier threshold greater than 0.5, 1.0, and 1.5.

DISCLAIMER

This report was prepared as an account of work sponsored by an agency of the United States Government. Neither the United States Government nor any agency thereof, nor any of their employees, makes any warranty, express or implied, or assumes any legal liability or responsibility for the accuracy, completeness, or usefulness of any information, apparatus, product, or process disclosed, or represents that its use would not infringe privately owned rights. Reference herein to any specific commercial product, process, or service by trade name, trademark, manufacturer, or otherwise does not necessarily constitute or imply its endorsement, recommendation, or favoring by the United States Government or any agency thereof. The views and opinions of authors expressed herein do not necessarily state or reflect those of the United States Government or any agency thereof.